UCRL-JRNL-216250

Extending ion-track lithography to the low-energy ion regime

R. G. Musket

October 18, 2005

Journal of Applied Physics

Disclaimer

This document was prepared as an account of work sponsored by an agency of the United States Government. Neither the United States Government nor the University of California nor any of their employees, makes any warranty, express or implied, or assumes any legal liability or responsibility for the accuracy, completeness, or usefulness of any information, apparatus, product, or process disclosed, or represents that its use would not infringe privately owned rights. Reference herein to any specific commercial product, process, or service by trade name, trademark, manufacturer, or otherwise, does not necessarily constitute or imply its endorsement, recommendation, or favoring by the United States Government or the University of California. The views and opinions of authors expressed herein do not necessarily state or reflect those of the United States Government or the University of California, and shall not be used for advertising or product endorsement purposes.

Extending ion-track lithography to the low-energy ion regime

R. G. Musket[a)]
Lawrence Livermore National Laboratory, Livermore, CA 94550

Abstract

Ion tracking and ion-track lithography have been performed almost exclusively using ions with energies near or above the maximum in electronic stopping, which occurs at ~1 MeV/amu. In this paper, ion-track lithography using ions with energies well below this maximum is discussed. The results of etching ion tracks created in polycarbonate films by ions with energies just above the anticipated threshold for creating etchable latent tracks with cylindrical geometry have been examined. Low-energy neon and argon ions with 18-60 keV/amu and fluences of $\sim 10^8/cm^2$ were used to examine the limits for producing useful, etchable tracks in polycarbonate films. By concentrating on the early stages of etching (i.e., ~20 nm < SEM hole diameter < ~100 nm), the energy deposition calculated for the incident ion was correlated with the creation of etchable tracks. The experimental results are discussed with regard to the energy losses of the ions in the polycarbonate films and to the formation of continuous latent tracks through the entire thickness of the films. The probability distributions for large-angle scattering events were calculated to assess their importance as a function of ion energy. All these results have significant implications with respect to the threshold for formation of etchable tracks and to the use of low-energy ions for lithographic applications of ion tracking.

a)Present address: Musket Consulting, El Dorado Hills, CA 95762; musket6@aol.com

I. INTRODUCTION

Nuclear, or ion, tracking has been the subject of considerable scientific interest and technological applications.[1-5] Lithographic applications of ion tracking have been recognized for over fifteen years,[3] but the main uses have been for fabricating simple filters with very small diameter holes and for creation of molds for electrodeposition of long, cylindrical or faceted structures (or nanocolumns) into the etched track holes. By using etched tracks in a polycarbonate film as the initial mask for the creation of an array of gated, field-emission cathodes, we extended the lithographic applications of ion tracking to more complicated structures.[6] For this case and for the creation of simple nanocolumn field emitters,[7,8] we used ~0.1 MeV/amu xenon ions to create the tracks, but we had interest in lowering the ion energy and atomic number to enable the lithography with smaller and less costly tracking equipment. Considerations for such low-energy ion-track lithography is the main topic of this paper. The results of etching ion tracks created in polycarbonate films by ions with energies just above the anticipated threshold for creating useful, etchable latent tracks with cylindrical geometry have been examined. In addition, calculations assessing the importance of large-angle scattering events on the application of such low-energy ions to lithography are also presented. As background, the discussion below gives the essence of the track formation process, summarizes the relevant literature on tracking polycarbonate foils, and defines our study.

I.A. Track formation processes

As an ion slows in a material, it loses energy by inelastic interactions with the electrons (electronic losses or electronic stopping) and, at sufficiently low velocities, by elastic collisions with the atoms (nuclear losses or nuclear stopping). Ion tracks resulting

from electronic stopping lead to well-defined structures suitable for lithography. When the ion velocity is sufficiently high, the ion trajectory is essentially a straight line along its path because the ions interact mainly with the electrons of the material. Due to statistical fluctuations in the energy deposition, continuous volumes of extended defects in the material can only be expected for high levels of energy deposition. As the electronic stopping power increases, the damage morphology for $Y_3Fe_5O_{12}$ changes from (a) isolated spherical defects to (b) overlapping of spherical defects to form longer discontinuous cylindrical defects to (c) continuous cylindrical defects.[9] The most well-defined latent ion tracks (i.e., tracks that exist prior to etching) are those that consist of such continuous cylindrical defects centered on the essentially straight ion path. A similar progression of track morphology has been reported for a polyimide (Kapton).[10,11] Furthermore, the effective damage radius for $Y_3Fe_5O_{12}$ has been shown[12] to be dependent on both the electronic stopping and the ion velocity with damage cross-section for a given value of electronic stopping being greater for lower velocity ions. They explained this effect by the energy deposition being more localized for the low-velocity ions than for the high-velocity ions. This experimental result is consistent with early calculations for plastics indicating that etchable tracks are formed when the deposited energy density near the ion path exceeds a critical value, which is characteristic of the material.[13]

I.B. Tracking and etching polycarbonate

For more than thirty years, polycarbonate foils have been used as particle detectors and in tracking studies.[1-5] The chemical formula for polycarbonate is $[(OC_6H_4)C(CH_3)_2(C_6H_4O)C)]_n$ or $C_{16}H_{14}O_3$, and it has the structure shown in Fig. 1.[14]

The two main commercially available versions of polycarbonate are Lexan and Makrofol, but polycarbonates with the same chemical composition manufactured by different chemical processes have been shown to have slightly different etching behavior after tracking.[15]

Many studies have been undertaken to understand the details of the damage and the enhanced etching rates in the latent tracks (e.g., the nature and reactivity of the chemical species created). Identification of various radiolysis products (pairs of free radicals) and interpretation of the enhanced etching in tracks in bisphenol-A polycarbonate have been made using thermoluminescence[12] and electron spin resonance.[14, 16-18] In essence, non-tracked polycarbonate is etched by chemical cleavage of the carbonate linkage by hydroxide with hydrolysis of two adjacent carbonate linkages being required to release the relatively soluble bisphenolate anion from the surface.[19] The chain scissions existing in the latent tracks result in monomer segments at the end of a chain and require only one chemical cleavage. This simpler process contributes to the higher etch rate in the track. In addition the etchant can diffuse faster into the track than into the non-tracked material. A combination of these effects qualitatively explains the much higher etch rates for the tracks compared to the non-tracked material.

The stability of latent tracks and their susceptibility to etching can be enhanced by exposure to ultraviolet (UV) radiation in air or oxygen.[19,20-22] A probable explanation of this enhancement has been proposed.[19] Oxygen reaction with radical or excited phenolic groups could occur in the absence of UV, while in the presence of UV, normal phenol groups would also react. In addition, such UV exposures in the presence of oxygen enhance the long term stability of the scissions.

When latent tracks are created in polycarbonate using heavy, high-velocity ions that deposit very large amounts of energy into electronic excitation, the etching rate in the track v_T is orders of magnitude greater than that of the non-tracked material v_G (G signifies the material in general), indicating that the latent track can be described as a cylinder of continuous bond scission damage. For simple chemical etching in 3N NaOH, a v_T/v_G ratio of 390 has been measured for fission fragments.[22] A 30-minute, post-irradiation exposure to UV in air yielded a v_T/v_G ratio of 10,300 (a factor of ~26 enhancement) for the same irradiation and etching conditions. Both v_T and v_G have a temperature dependence that follows the Arrhenius equation with the v_T/v_G ratio decreasing with temperature due to the higher activation energy of v_G.[15]

Chemical etching of a cylindrical latent track leads generally to a conically shaped hole with the base of the cone at the surface of the material.[1-4] The sine of the cone half angle is equal to v_G/v_T. Thus, if $v_T/v_G = 390$ (as above), the cone half angle would be ~0.15 degrees, and the etched hole could be described as having a cylindrical shape. For many lithographic applications, the etched hole does not need to be truly cylindrical, and a somewhat cylindrical shape (i.e., a slightly tapered hole) would be acceptable. Such a shape results when $v_T/v_G \geq 10$, because the cone half angle would be ≤ 5.7 degrees. For a 1 μm thick film on a substrate, a 5.7-degree cone angle would lead to an etched hole diameter at the top of the film being about 200 nm greater than that at the bottom of the film. This type of tapered hole may be acceptable for many lithographic applications; thus, assessing the threshold required to give $v_T/v_G = 10$ is a reasonable benchmark.

In addition to etching long holes in materials, the continuous nature of the latent tracks can be assessed by determining the registration efficiency for the ions of interest.

If the latent tracks are essentially continuous, then, after a short etching period, the etched track density (tracks/cm^2) will equal the ion fluence (ion/cm^2) (i.e., 100% registration efficiency) and both the lengths and the diameters of the etched tracks will be identical. High values of v_T/v_G are correlated with high values of energy deposition and of registration efficiency.[23] Cases where v_T is only slightly greater than v_G (i.e., $v_T/v_G = 1+\delta$, where $\delta << 1$) correspond to a non-continuous latent track with regions of scissions separated by regions without scissions. Such sporadic scission damage along the ion path leads to lower registration efficiency and greater variation of the etched lengths and diameters. Thus, cases with $v_T/v_G = 1+\delta$ correspond to a registration efficiency near zero.

The stopping, or energy loss rate curves for Xe, Ar, and Ne ions in polycarbonate as a function of reduced energy (MeV/amu) are shown in Fig. 2. These curves were calculated using the SRIM (i.e., Stopping and Range of Ions in Matter) code.[24] The maximum loss rates for these three ions (i.e., the Bragg peaks) are 88 MeV cm^2/mg at 2.1 MeV/amu for Xe, 29 MeV cm^2/mg at 0.69 MeV/amu for Ar, and 15 MeV cm^2/mg at 0.45 MeV/amu for Ne. At these peaks the ratios of electronic to nuclear stopping are 434, 428, and 468, respectively. Thus, for ions with energies near these peak stopping values, essentially all the energy deposition is due to electronic excitation. At energies below the Bragg peak the importance of nuclear stopping increases. Each stopping value below the Bragg peak intersects the electronic stopping curve at two different energies, termed the lower and upper energies.

I.C. Track threshold considerations

Over the years different approaches have been suggested to relate some aspect of the deposited energy with the threshold for creating continuous latent tracks. The

original interest in knowing the threshold was to permit correlation of the observed lengths of etched tracks in a material with those calculated, as a function of ion species and ion energy. Thus, the emphasis was on determining the etching threshold (i.e., the minimum energy deposition rate that leads to etchable tracks). Our interest is in determining the minimum energy required for a specific ion to create a continuous latent track with $v_T/v_G \geq 10$ throughout the thickness of a polycarbonate resist layer. As mentioned above, such tracks should be suitable for lithography. The main approaches to relating the experimental results to the stopping of the ions have been total energy loss, restricted energy loss, and thermal spike.

Initially, the threshold criterion for creating continuous latent tracks was believed to be the minimum required total stopping,[25] which is dominated by electronic stopping (abbreviated as SE) at the upper energies. Another method to relate the energy deposition rate to the threshold for track formation is the restricted energy loss (i.e., REL) method.[13] The REL includes only that portion of the total energy loss that produces delta rays (i.e., electrons) of less than some specified energy (usually < 350 eV or < 1 keV) that deposit their energy near the ion path. Because this method relies on a calculation of both the electronic stopping and the energy distribution of electrons, there is additional uncertainty in the calculation compared to the total electronic stopping method. For ions with energies well below the Bragg peak the electron energies are smaller and the REL approach should give results similar to that of the SE approach. Typically, the threshold has been determined by measuring the track etch rate as a function of the REL. The threshold REL has been evaluated by extrapolation of the data to $v_T/v_G = 1$.

For ions with energies well below the Bragg peak, the REL threshold determined in this way corresponds to very low energy ions that deposit their energy mainly into elastic atomic displacements resulting in damage clusters of various sizes. These very low energy ions cause radiation damage and chain scission, but only at the surface; thus, slightly enhanced etching rates are observed only for very shallow depths. Detection of such "tracks" at surfaces of non-etched or very slightly etched material leads to the smallest values for the threshold. However, such "tracks" are not useful for ion tracking lithography because of their shallow depths and non-uniform sizes and will not be discussed further here.

In recent years, the concept of a thermal spike model has been quantified and applied to a variety of ion and material combinations, but has not been applied to polycarbonate.[9,12,26-28] These calculations assume that the latent tracks result from a transient thermal process. The elevated temperatures along the path of the ion result from the transfer of energy of the ion-excited electrons to the nearby atoms. Because the electron-lattice coupling is better in insulating materials than in metals, a larger increase of temperature along the ion trajectory is expected in insulating materials.[27] However, this model has not been applied to polymers because of the more complex nature of the radiolytic degradation processes.[28] Thus, the thermal spike model probably not directly applicable to tracking in polycarbonate. ESR results for polycarbonate indicated that production of free radicals directly by electrons rather than by thermal spikes explain the formation of latent tracks; this conclusion was established by the observation that the nature of the free radicals was independent of the type of incident particle (gamma, electron, neutron, or ion).[18]

A summary of the relevant literature for the three threshold methods applied to polycarbonate materials is given in Table 1. From this table, we can draw two main conclusions: (a) 100% registration has been reported for SE = 5.5 to 8 MeV cm^2/mg and REL = ~3 MeV cm^2/mg; and (b) for the v_T/v_G = 10 criterion, SE = 9 to 16 MeV cm^2/mg and REL = 5 to 10.6 MeV cm^2/mg. The large variations in the results from different studies are presumably a result of some combination of the following: (a) slightly different materials and levels of surface cleanliness, (b) variation in the amount of incidental exposure to UV radiation after tracking, (c) different etching conditions (etchants and temperatures), and (d) different methods of calculating REL and SE. As indicated in Table 1, controlled air exposure of the tracked Lexan to UV radiation markedly reduced the thresholds for etching.[21] This UV exposure decreased the v_T/v_G = 1 and v_T/v_G = 10 thresholds by more than a factor of two. Because SE approaches REL for the low energy ions of interest here (due to the low energies of the excited electrons), a reasonable assumption is that the SE threshold for useful lithography can be approximated by the REL threshold for v_T/v_G = 10, which is in the range of 4.3 to10.6 MeV cm^2/mg without UV exposure prior to etching, but as low as 3.4 MeV cm^2/mg with UV exposure.

I.D. Definition of study

As seen in Fig. 2, the ratio of electronic to nuclear stopping decreases rapidly with ion energies below the Bragg peak. As examples, for 13.6-MeV Xe (~0.10 MeV/amu) and 2-MeV Ar (~0.05 MeV/amu) the ratios of electronic to nuclear stopping are 11 and 21, respectively. These ratios are much less than the corresponding peak ratios of 434 and 428. Nevertheless, 13.6-MeV Xe has been used successfully for ion track

lithography on 0.6-μm thick polycarbonate films.[6-8] Our goal was to demonstrate that much lower-energy, lighter ions can be used to perform the lithography through such films, and, consequently, reduce the tracking equipment requirements to something similar to standard ion implanters that have lower high-voltage terminals and smaller analyzing magnets than the accelerator systems normally used for ion tracking. In particular, we were interested in reducing the ion energy and mass from the 13.6-MeV Xe ions that we previously used for ion track lithography in 600-nm thick Makrolon films[6-8] and in increasing the film thickness to at least 1 μm.

Considerations of the results of Table 1, the curves of Fig. 2, the ion ranges for energies of interest, and limited resources led to the decision to limit the study to the SE (or REL) range of 6 to 8 MeV cm^2/mg using low-energy neon and argon ions (i.e., 18-60 keV/amu) with pre-etching exposure to UV radiation in air. This SE range is above the expected threshold of 3.4 MeV cm^2/mg for pre-etching exposure to UV radiation in air.[21] The basic idea was to verify the expected formation of useful, etchable latent tracks by registration after minimal etching and uniform hole sizes after longer etching times. Assuming this expectation was true (for at least part of the SE range of 6 to 8 MeV cm^2/mg), the ion energy corresponding to the lowest effective SE could be taken as an energy that the ion must have at the film/substrate interface (after passing through the polycarbonate film). Under this interface condition, the stopping curves could be used to determine the required incident ion energy for etching of a nearly cylindrical hole throughout the thickness of a polycarbonate film.

At lower ion energies the nuclear stopping increases, and large-angle scattering events become more important. Such scattering effects must be evaluated for ion-track

lithography applications, because they can result in nonlinear ion paths and, thus, non-linear holes etched through the film. Using the SRIM code, the angular distributions of ions that passed through polycarbonate foils of various thicknesses were calculated, and assessment of the importance of large-angle scattering events was made.

II. EXPERIMENTAL CONSIDERATIONS

Using SRIM we determined the energies of the Ne and Ar ions required to deposit SE values of about 6, 6.5, 7, 7.5, and 8 MeV cm^2/mg as the ion entered the surface of the polycarbonate. The required energies were 0.80, 0.90, 1.00, 1.10, and 1.20 MeV for Ne and 0.70, 0.82, 0.94, 1.05, and 1.16 MeV for Ar. In addition, we included tracking with 2 MeV Ar, which initially deposits an SE ~ 11 MeV cm^2/mg (Fig. 2b), and 13.6-MeV Xe, which initially deposits SE ~ 22 MeV cm^2/mg (Fig. 2a). Tracking with 2-MeV Ar was considered to be an initial goal that allowed lowering the ion energy and atomic number to enable the lithography with smaller and less costly ion-accelerator equipment; however, we needed to determine that the energy of the Ar at the film/substrate was sufficient to create useful, etchable tracks. Results for 13.6 MeV Xe that had been used in our previous ion-track lithography studies,[6-8] have been included for comparison.

Makrolon polycarbonate films (~600-nm thick) were deposited onto 100-mm diameter, chromium-coated glass substrates using deposition and baking procedures similar to those previously reported.[6] A 50 mm X 50 mm square near the center of the 100-mm diameter substrate was irradiated using a magnetically analyzed, electrostatically rastered beam of Ne^+, Ar^+, or Xe^{+4} ions using a 4-MV single-ended accelerator with a cold cathode ion source. The ions were incident along the surface normal (±2°). Typical beam currents were 0.1 to 7.0 nA with the dosimetry being determined by the average

fluence received in an array of four Faraday cups located outside the corners of a 50 mm X 50 mm aperture carbon mask in front of the substrates. Electronically measured fluence values were (1 ± 0.05) X 10^8 atoms/cm^2.

The uniformity of the irradiations was achieved by rastering the approximately 1 cm diameter beam over an area greater than the 50 mm X 50 mm aperture for a minimum of 10 s and was then assessed by comparing the fluence collected in each of the four Faraday cups inside the corners of the rastered area. The maximum deviation in any one cup from the average fluence in the four cups during the irradiations was <5%. The area having latent tracks was uniformly exposed to 205 nm, UV radiation in air for about 15 minutes with a power of 20 mW/cm^2. Etching of the ion-irradiated and UV-exposed polycarbonate films was accomplished in a 6 M solution of high-purity potassium hydroxide (KOH) for various times at a temperature of about 22 C. Multiple etching experiments were made on the same irradiated film by using a glass tube with an o-ring at the end to limit each etching to a circular area of about 38 mm^2. The etching times were generally 1, 2, 4, 6, 8, and 10 minutes for each irradiated film. Etching was stopped by removal from the KOH solution and rinsing in de-ionized water.

III. RESULTS AND DISCUSSION

III.A. Tracking and etching studies

Images of the etched holes (after depositing a thin coating of carbon) were obtained as a function of etching time using low-energy SEM at near normal incidence. The cylindrical hole diameter was taken to be the diameter of the dark hole as determined using the calibrated markers in both the X and Y directions of the micrograph. An example of this measurement scheme is shown in Fig. 3. A sequence of SEMs showing

the effects of increasing the etching time from one to eight minutes is displayed in Fig. 4. The indicated hole diameters were determined using SEMs with magnifications 1.67 times those in Fig. 4.

Although the largest percentage errors occur for the smallest hole diameters, no effort has been made to assess such measurements errors as a function of hole diameter. The largest errors are believed to be associated with the reproducibility of the etching process parameters, including initial surface cleanliness, substrate and etchant temperature, and timing of the etch start and stop. In addition, the variability of the thicknesses of the thin carbon coatings was believed to be a contributor to errors for the smallest holes.

Uniform irradiation should have led to etched tracks densities (tracks/cm^2) equal to the measured fluences, indicating unity probability of track formation. For 13.6 MeV Xe ions, the etched hole densities were found using SEM to be 0.99 (± 0.05) X 10^8/cm^2, which agrees with the electronically measured fluence of 1.00 (± 0.05) X 10^8/cm^2. Unfortunately, the SEM fluences for the lower-energy ions were either equal to or greater than the measured fluences, indicating that there was some bombardment by neutralized ions, which were not measured by the dosimetry system. For example, the etched hole density for 2 MeV Ar ions was 1.22 (± 0.11) X 10^8/cm^2. Consequently, we could not draw any firm conclusions about the track registration efficiency of these ions, but the uniform hole sizes for the 2 MeV Ar case is indicative of the damage in the latent tracks being above the threshold for continuous cylindrical damage.

A comparison of the hole diameter as a function of etching time for 2 MeV Ar and 13.6 MeV Xe is given in Fig. 5. Recall that both these ions deposit energy well

above the threshold for creation of etchable tracks. The individual lines are linear-regression fits to the two sets of data. All six data points for Ar were used for the fitting, and eight data points from ref. 6 were used for fitting the Xe data. All eight points shown were those obtained after carefully re-evaluating the hole diameters using the original SEMs, but only hole diameters for the 1 and 1.5 minute etchings were found to be different from those in ref. 6. The sample preparation, the UV exposure, and the etching procedure in this study was similar to that of ref. 6.

R^2 is a measure of the reliability of the fit with $R^2 = 1$ being a perfect fit; thus, both sets of data in Fig. 5 are well fit by a straight line. Extrapolations of these fits to zero time suggest latent track diameters of about 16 nm for the Xe and 3 nm for the Ar. However, these values are upper limits on the diameter for the latent tracks, which initially etch very rapidly. Due to the quite different ions and SE values, the extrapolated hole sizes at zero etching time were not expected to be the same. However, the slopes of the two lines were expected to be nearly the same, because the increase of the hole diameter with etching time should have been similar. The fitted line for Xe has a slope that is ~17 % less than that for Ar; this variance is presumably a consequence of using slightly different samples, UV exposures, and etching procedures. This figure clearly shows that both 13.6 MeV Xe and 2 MeV Ar are effective in creating etchable tracks in polycarbonate with similar time dependencies for the etched hole diameters.

Some initial studies of the dependence of the etched hole diameter on Ar energy (0.7-2 MeV) with etching time as a parameter were completed. All of these ions created etchable tracks, and the etched hole diameters generally increased with etching time for each Ar energy. For Ar energies of 0.7-1.16 MeV, the hole diameter for each etching

time was essentially independent of Ar energy. For etching times greater than 2 minutes, the etched hole diameters for 2-MeV Ar were larger than those for all other energies.

We repeated some of the etching procedures on all five of the low energy Ar cases for a total of fourteen repeat etchings. For four cases the results changed from no detectable holes to holes with measurable diameters. In one case the results changed from measurable holes to no detectable holes. For the nine other cases, the reproducibility of the hole diameters varied from 0.5 % to 22 % with the average variation being ± 11 %. In some of these cases, there was a bimodal distribution of etched hole diameters. The reasons for these discrepancies are not clear, but issues related to the reproducibility of the etching process parameters, especially surface cleanliness, are suspected.

Similarly, some initial studies of the dependence of the etched hole diameter on Ne energy (0.8-1.2 MeV) with etching time as a parameter were completed. As with the Ar ions above, all of these Ne ions created etchable tracks and the hole diameter generally increased with etching time for each Ne energy. In agreement with the low-energy Ar data, the etched hole diameter did not change significantly with Ne energy, and the low-energy Ne and Ar irradiations resulted in similar hole sizes for the same etching time.

Although additional experiments with lower energy Ar and/or Ne ions are needed to actually determine the threshold for creation of etchable tracks, we have verified that the SE threshold for $v_T/v_G = 10$ is < 6 MeV cm^2/mg, as expected. Thus, Ar ions should be suitable for ion track lithography of polycarbonate films in all cases where the Ar deposits more than this threshold amount of energy in the film at the film/substrate

interface after the ion has lost energy in passing through the film. From SRIM calculations, a 2 MeV Ar ion incident on the 600-nm thick polycarbonate film would have its energy reduced to about 1.23 MeV at the film/substrate interface where it would deposit about 8.28 MeV cm^2/mg. Using the 6 MeV cm^2/mg as the required SE at the film/substrate interface, SRIM calculations for 2, 1.8, and 1.6 MeV Ar showed that the trackable thicknesses are 1.15, 1.01, and 0.86 μm, respectively.

In Fig. 6(a) the etched holes can be seen to be quite uniform in size. To verify that the 107-nm diameter holes found were really cylinders throughout the thickness of the film, we prepared cross-sectional samples for SEM analysis by pulling the film off in some areas. The micrographs shown in Fig. 6(b) and 6(c) were taken at different locations along tear lines to show the general features. As expected the holes are nearly cylindrical in shape throughout the thickness of the film. After examining many cross-sectional areas, we could only find cylindrical holes; there was no evidence of holes that did not penetrate the film. The oscillations in the diameters of the holes throughout the thickness of the film are due presumably to the enhanced sensitivity to etching created by the standing wave pattern due to the UV radiation interacting with the film.[35] Using several different SEMs and correcting for the sample tilt angle (~30°), the thickness removed from the top by etching was ~80 nm, which, as expected, is comparable to the etched hole radius of ~54 nm.

III.B. Calculations of large-angle scatterings

As the ion energy decreases below that of the Bragg peak, the ratio of electronic stopping to nuclear stopping decreases (Fig. 2), and the importance of the large angle scattering of the ions (caused by elastic nuclear scattering) increases relative to the

extremely small angle scatterings during inelastic electron scattering. The kinematics of elastic scattering from H, C, and O limits the maximum, respective scattering angles to 1.43, 17.45, and 23.57 degrees for Ar ions and to 0.43, 5.24, and 6.99 degrees for Xe ions. These angles are sufficiently large to require assessment of the effects of scattering of these ions before using them to perform ion-track lithography.

Monte Carlo calculations (SRIM2000.39[24]) were used to evaluate the effect of large-angle scattering events within the film by calculating the exit angles for ions entering into a free-standing foil along the normal to the foil surface. Each calculation was performed with a minimum of 10,000 ions. The composition of the foil was taken to be that of polycarbonate ($C_{16}H_{14}O_3$) with a density of 1.20 g/cm^2. The default SRIM stopping correction of 1.054 was adopted for these calculations. SRIM provides a file named TRANSMIT.TXT that provides, among other results, the three direction cosines of the exit angles, which were used to determine the exit angle of each ion. The resulting probability distributions for the differential and integral fraction of ions have been plotted as a function of the exit angle.

For 1-µm thick polycarbonate layers and 30,000 ion histories, the exit angles calculated for 2-MeV Ar ions have been compared with those for the 13.6-MeV Xe ions in Fig.7. For Xe the average exit angle was 1.97 ± 0.98 degrees with the maximum exit angle being < 5 degrees. Such scattering effects were certainly acceptable for our applications. In contrast, the average exit angle for Ar was 6.54 ± 3.30 degrees with only 83 % of the ions exiting at angles < 10 degrees. Such large scattering angles cause a strong deviation from the straight track desired for lithographic applications. Through etching of large-angle, non-linear latent tracks may not occur in the same time frame as

for straight-through tracks. Thus, the density and the size distribution of etched track holes on the exit side of the film may be less than that on the entrance side. Examination of .the etched holes in Fig. 6(a) reveals a non-circular hole at the upper left corner. This hole could have resulted from a large angle scattering event near the top of the film

As shown in Fig. 8, decreasing the film thickness from 1 µm to either 0.8 µm or 0.6 µm decreases the integral fraction of ions with large angles. For 0.6 µm thick films, >95 % of the Ar ions exit with angles < 10 degrees. For our applications this is probably acceptable, but more experiments are required to confirm this conclusion.

For 1-µm thick layers, the exit angles for 2 to 6 MeV Ar ions were calculated (Fig. 9). The angle below which about 95 % of the Ar ions exit decreases from < 15 degrees at 2 MeV to < 10 degrees at 3 MeV to < 5 degrees at 6 MeV. This is simply a consequence of the decreasing importance of nuclear stopping with Ar ion energy. The result for 6 MeV Ar is certainly acceptable for our applications.

IV. SUMMARY AND CONCLUDING REMARKS

We have examined the results of etching ion tracks created by ions bombarding polycarbonate films with energies corresponding to electronic stopping power (SE) just above the anticipated threshold for creating etchable latent tracks. Low-energy neon and argon ions with 18-60 keV/amu were used to examine the limits for producing etchable tracks in polycarbonate films, and the results were compared to our previous work with 13.6 MeV Xe (~100 keV/amu).[6-8] Although additional experiments with lower energy Ar and/or Ne ions are needed to actually determine the threshold for creation of etchable tracks, we have confirmed that the SE threshold is <6 MeV cm^2/mg. Furthermore,

improved control of the etching parameters should permit higher reproducibility of the etching studies and better assessment of any trends with low ion energies.

Using cross-sectional SEM we found that an energy deposition of about 8.28 MeV cm^2/mg in the polycarbonate at the film/substrate interface is sufficient to ensure that the etched hole will be nearly cylindrical in shape throughout the film thickness. Under the assumption that the threshold for creating etchable latent tracks in polycarbonate is conservatively 6 MeV cm^2/mg, SRIM was used to calculate the maximum thickness of polycarbonate film that can be tracked using Ar ions of various energies. For 2, 1.8, and 1.6 MeV Ar the trackable thicknesses are 1.15, 1.01, and 0.86 μm, respectively. However, at lower energies the effect of the nuclear stopping increases and higher angle scattering events become more important. The present results have significant implications with respect to the threshold for formation of etchable tracks and to the use of low-energy ions for lithographic applications.

ACKNOWLEDGMENTS

It is a pleasure to acknowledge R. J. Contolini for initial discussions of this work, the late R. G. Patterson for doing most of the irradiations, L. A. Tarte for performing the etching experiments, and J. M. Yoshiyama for the SEM measurements, and A. Johnson of Candescent Technologies Corporation for the preparation of the samples. Great appreciation is extended to T. E. Felter for a critical review of the manuscript and a continuing interest in this work. Work performed under the auspices of the U. S. Department of Energy by UC, Lawrence Livermore National Laboratory under contract W-7405-ENG-48, including CRADA TC-774-94 with Candescent Technologies Corporation.

References

1. R. L. Fleischer, P. B. Price, and R. M. Walker, *Nuclear Tracks in Solids: Principles and Applications* (University of California Press, Berkeley, CA, 1975).

2. S. A. Durrani and R. K. Bull, *Solid State Nuclear Track Detection: Principles, Methods, and Applications* (Pergamon Press, New York, 1987).

3. R. Spohr, *Ion Tracks and Microtechnology: Principles and Applications* (Vieweg, Braunschweig, Germany, 1990)

4. R. L. Fleischer, *Tracks to Innovation: Nuclear Tracks in Science and Technology* (Springer-Verlag, New York, 1998)

5. W. Enge, Rad. Meas. **25**, 11 (1995).

6. A. F. Bernhardt, R. J. Contolini, A. F. Jankowski, V. Liberman, J. D. Morse, R. G. Musket, R. Barton, J. Macaulay, and C. Spindt, J. Vac. Sci. Technol. B **18**, 1212 (2000).

7. R. G. Musket, Mat. Res. Soc. Symp. Proc. **621**, R1.2.1 (2000).

8. T. E. Felter, R. G. Musket, J. Macaulay, R. J. Contolini, and P. C. Searson, Mat. Res. Soc. Symp. Proc. **777**, 121 (2003).

9. M. Toulemonde and F. Studer, Diffusion and Defect Data: Solid State Phenomena **23 & 24**, 161 (1992).

10. C. Trautmann, Nucl. Instr. and Meth. B **105**, 81 (1995).

11. C. Trautmann, S. Bouffard, and R. Spohr, Nucl. Instr. and Meth. B **116**, 429 (1996).

12. A. Meftah, F. Brisard, J. M. Costantini, M. Hage-Ali, J. P. Stoquert, F. Studer, and M. Toulemonde, Phys. Rev. B **48**, 920 (1993).

13. E. V. Benton and W. D. Nix, Nucl. Instr. and Meth. **67**, 343 (1969).

14. E. A. Edmonds and S. A. Durrani, Nucl. Tracks **3**, 3 (1979).

15. A. Kumar and R. Prasad, Rad. Meas. **31**, 227 (1999).

16. S. L. Koul and I. D. Campbell, Rad. Eff. **97**, 321 (1986).

17. E. Ferain and R. Legras, Rad. Eff. Def. Solids **126**, 243 (1993).

18. M. I. Chipara, V. V. Grecu, P. V. Notingher, J. R. Romero, and M. D. Chipara, Nucl. Instr. and Meth. B **88**, 418 (1994).

19. T. A. Gruhn and E. V. Benton, in *Solid State Nuclear Track Detectors*, P. H. Fowler and V. M. Clapham (eds) (Pergamon, New York, 1981), p. 69.

20. E. V. Benton and R. P. Henke, Nucl. Instr. And Meth. **70**, 183 (1969).

21. R. P. Henke, E. V. Benton, and H. H. Heckman, Rad. Eff. **3**, 43 (1970).

22. W. DeSorbo, Nucl. Tracks **3**, 13 (1979).

23. R. L. Fleischer, in *Progress in Materials Science* (*Chalmers Anniversary Issue*), J. W. Christian, P. Haasen, and T. B. Massalki (eds) (Pergamon Press, New York, 1981), p.97.

24. J. F. Ziegler, J. P, Biersack, U. Littmark, *The Stopping and Range of Ions in Solids*, vol. **1** of series *Stopping and Ranges of Ions in Matter* (Pergamon Press, New York, 1984) and J. F. Ziegler, www.srim.org.

25. R. L. Fleischer, P. B. Price, R. M. Walker, and E. L. Hubbard, Phys. Rev. **133**, 1443 (1964).

26. M. Toulemonde, E. Paumier, and C. Dufour, Rad. Eff. Def. Solids **126**, 201 (1993).

27. M. Toulemonde, C. Dufour, A. Meftah, and E. Paumier, Nucl. Instr. and Meth. B **166-167**, 903 (2000).

28. M. Toulemonde, C. Trautmann, E. Blaanzat, K. Hjort, and A. Weidinger, Nucl. Instr. and Meth. B **216**, 1 (2004).

29. M. Debeauvais, R. Stein, J. Ralarosy, and P. Cuer, Nucl. Phys. **A90**, 186 (1967).

30. G. Somogyi, K. Grabisch, R. Scherzer, and W. Enge, Nucl. Instr. and Meth. **134**, 129 (1976).

31. K. K. Dwivedi and S. Mukherji, Nucl. Instr. and Meth. **159**, 433 (1979).

32. S. M. Farid and A. P. Sharma, Ind. J. Pure Appl. Phys. **22**, 133 (1984).

33. G. Singh, S. Devi, S. Singh, and H. S. Virk, Nucl. Tracks **12**, 383 (1986).

34. S. Ghosh, A. Saxena, and K. K. Dwivedi, Pramana-J. Phys. (India) **31**, 197 (1988).

35. C. A. Mack, Appl. Optics **25**, 1958 (1986).

Table 1.
Literature values of critical energy deposition for track formation in polycarbonate

Material	Method used	Side of Bragg Peak	Ion Z Range	Critical energy deposition	Ref.
Lexan	100 % Registration	High	6 - 18	SE = 7 MeV cm^2 mg^{-1}	24
Lexan	100% Registration?	High & low	6 - 18	REL = 3.3 MeV cm^2 mg^{-1}	22
Makrofol E	100 % Registration?	High & low	10 - 18	SE = 5.5 to 8 MeV cm^2 mg^{-1}	29
Lexan	$v_T/v_G = 1$	High & low	6 - 18	REL = 2.0 MeV cm^2 mg^{-1} (<1 with UV)	21
"	$v_T/v_G = 10$	"	"	REL = 8.2 MeV cm^2 mg^{-1} (3.4 with UV)	"
Lexan, Makrofol E	$v_T/v_G = 1$	High & low	2 - 18	REL = 1 to 2 MeV cm^2 mg^{-1}	30
"	$v_T/v_G = 10$	"	"	REL = 5 to 8 MeV cm^2 mg^{-1}	"
Lexan	$v_T/v_G = 1$	High	FF	SE = 7.5 MeV cm^2 mg^{-1}	31
"	$v_T/v_G = 10$	"	"	SE = 13 MeV cm^2 mg^{-1}	"
Makrofol E	$v_T/v_G = 1$	High	8	SE = 4.9 MeV cm^2 mg^{-1}	32
"	$v_T/v_G = 9.5$	"	"	SE = 8.9 MeV cm^2 mg^{-1}	"
Makrofol	$v_T/v_G = 1$	High	54	REL = 4.3 MeV cm^2 mg^{-1}	33
"	$v_T/v_G = 10$	"	"	REL = 10.6 MeV cm^2 mg^{-1}	"
Lexan	$v_T/v_G = 1$	High & low	18	SE = 5.0 MeV cm^2 mg^{-1}	34
"	$v_T/v_G = 10$	"	"	SE = 16 MeV cm^2 mg^{-1}	"

Legend: SE = Total electronic stopping; REL = Restricted energy loss; FF = Fission fragments

.

Figure Captions

FIG. 1: Structural formula of polycarbonate (from ref 14).

FIG. 2: Calculated stopping of ions in polycarbonate: (a) Xe, (b) Ar, and (c) Ne.

FIG. 3: Typical SEM of etched holes in a polycarbonate film showing the calibrated spread between the cursors in the X and Y directions and hole diameters of about 151 nm (Conditions: 13.6 MeV Xe, UV/air exposed, 16 minutes of etching).

FIG. 4: SEMs showing growth of holes with etching time (after UV/air exposure) for polycarbonate films tracked by 13.6-MeV Xe: (a) 19 nm diameter after 1 minute, (b) 41 nm diameter after 2 minutes, (c) 56 nm after 4 minutes, and (d) 81 nm after 8 minutes.

FIG. 5: Dependence of the etched hole diameter on etching time after irradiation of polycarbonate with 2 MeV Ar and 13.6 MeV Xe.

FIG. 6: Holes etched in 600-nm thick polycarbonate films after irradiation with 2 MeV Ar ions and etching for 10 minutes: (a) top view SEM and (b&c) cross-sectional SEMs.

FIG. 7: Exit angles calculated for 13.6 MeV Xe and 2 MeV Ar incident along the surface normal of a 1-μm thick polycarbonate foil.

FIG. 8: Exit angles calculated for 2 MeV Ar incident along the surface normal of polycarbonate foils with various thicknesses.

FIG. 9: Exit angles calculated for various energies of Ar incident along the surface

normal of a 1-μm thick polycarbonate foil.

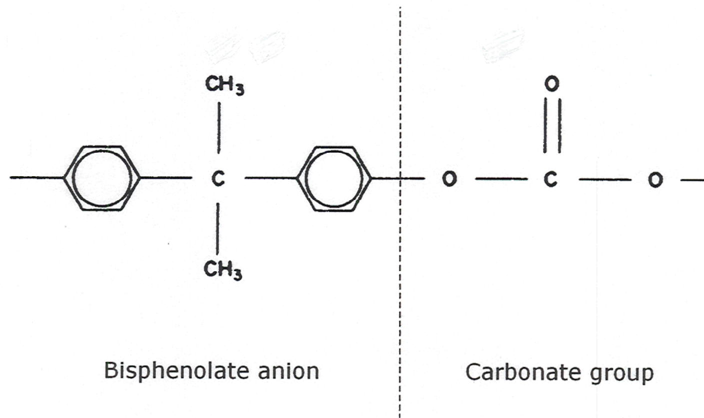

Figure 1: Structural formula of polycarbonate, $C_{16}H_{14}O_3$ (from ref. 14).

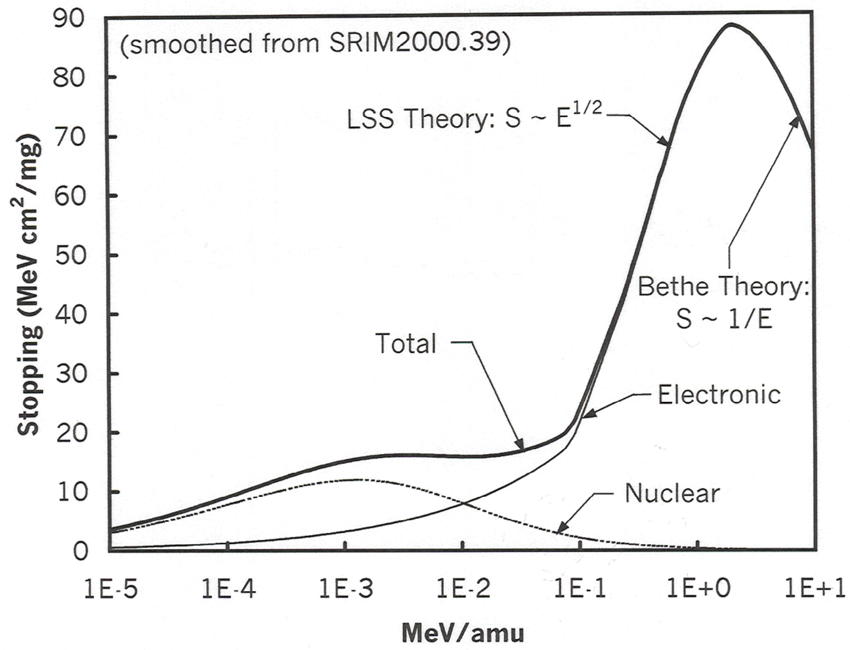

Figure 2(a): Calculated stopping of Xe in polycarbonate

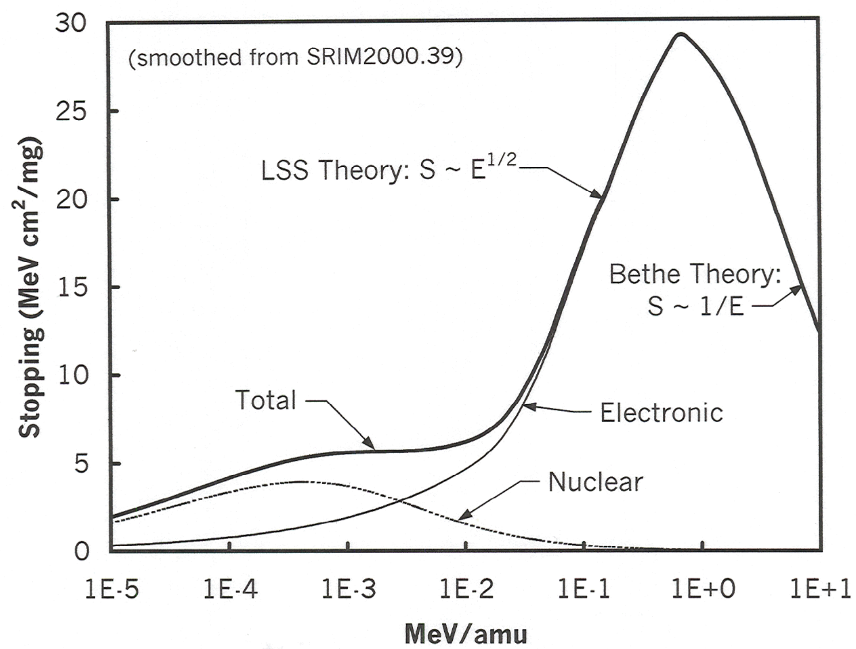

Figure 2(b): Calculated stopping of Ar in polycarbonate

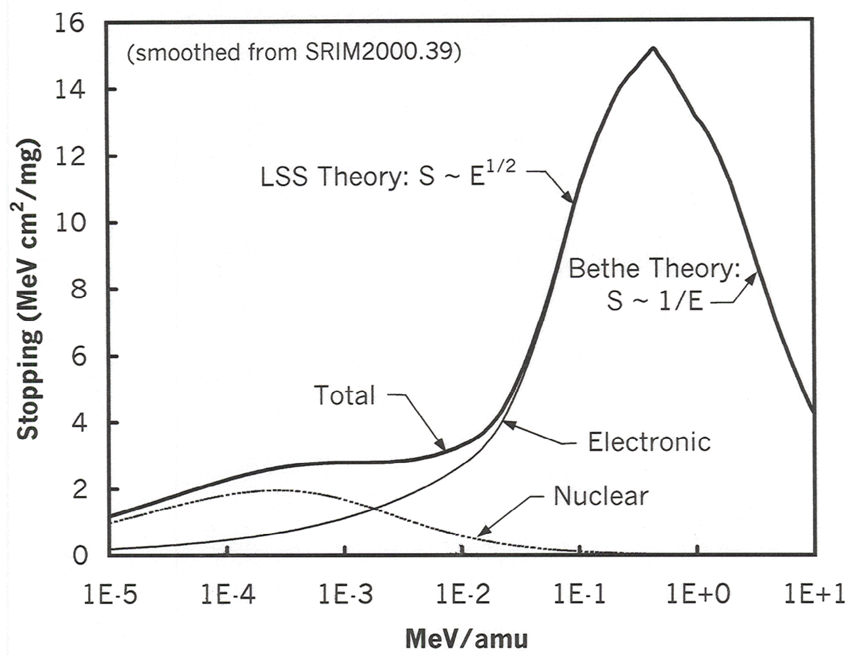

Figure 2(c): Calculated stopping of Ne in polycarbonate

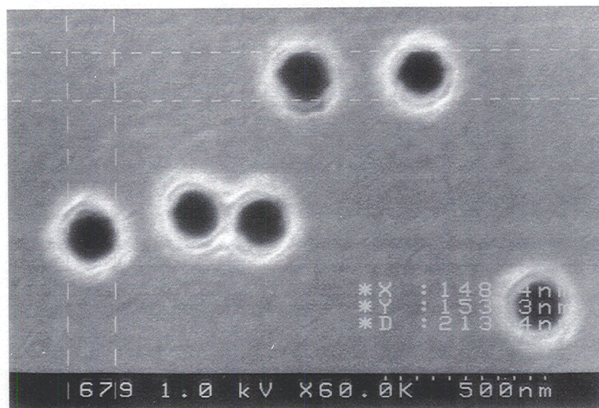

Figure 3: Typical SEM of etched holes in a polycarbonate film showing the calibrated spread between the cursors in the X and Y directions and hole diameters of about 151 nm (Conditions: 13.6 MeV Xe, UV/air exposed, 16 minutes of etching).

Figure 4(a)

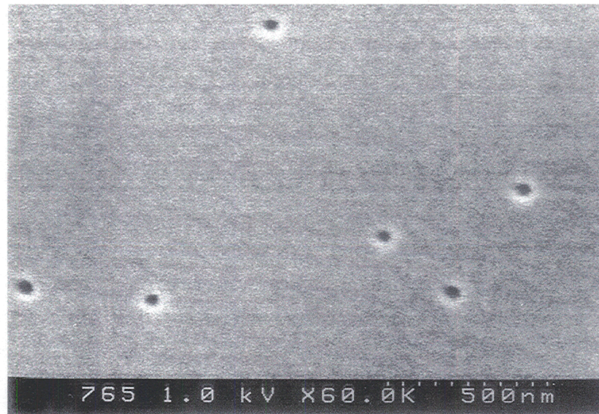

Figure 4(b)

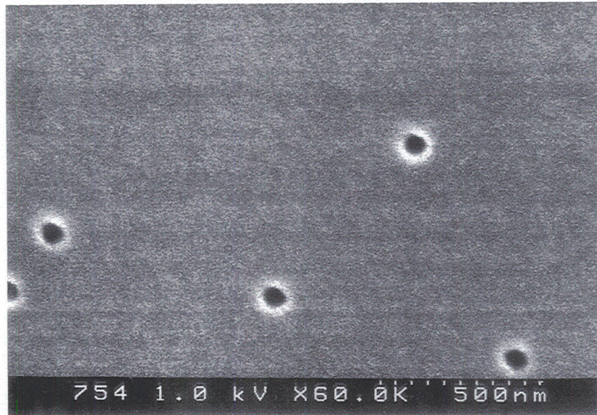

Figure 4(c)

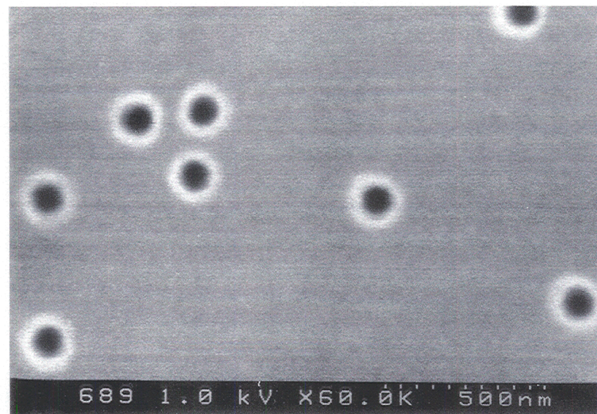

Figure 4(d)

Figure 4: SEMs showing growth of holes with etching time after UV/air exposure for polycarbonate films tracked by 13.6 MeV Xe ions: (a) 19 nm diameter after 1 minute, (b) 41 nm diameter after 2 minutes, (c) 56 nm after 4 minutes, and (d) 81 nm after 8 minutes.

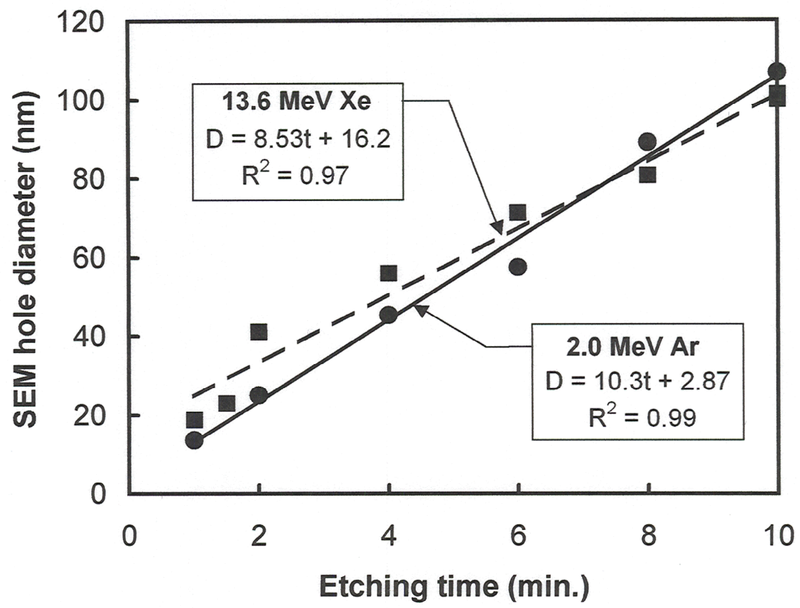

Figure 5: Dependence of the etched hole diameter on etching time after irradiation of polycarbonate with 2 MeV Ar and 13.6 MeV Xe.

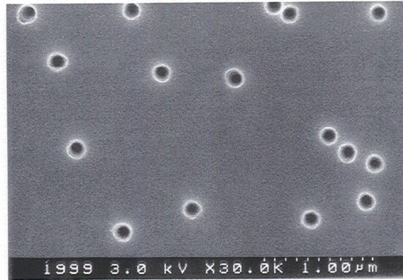

(a)

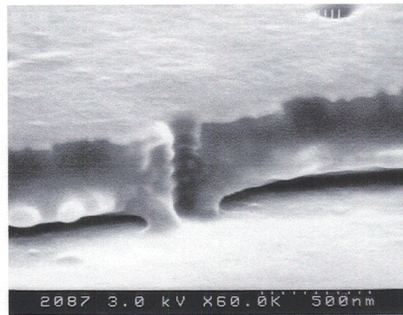

(b)

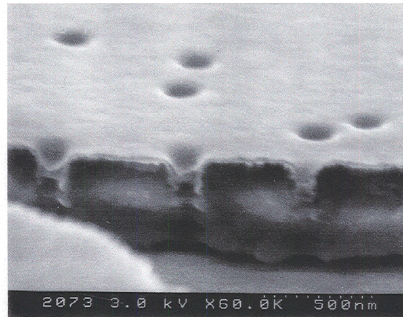

(c)

Figure 6: Holes etched in 600-nm thick polycarbonate film after irradiation with 2 MeV Ar ions and etching for 10 minutes (a) top view SEM and (b&c) cross-sectional SEMs.

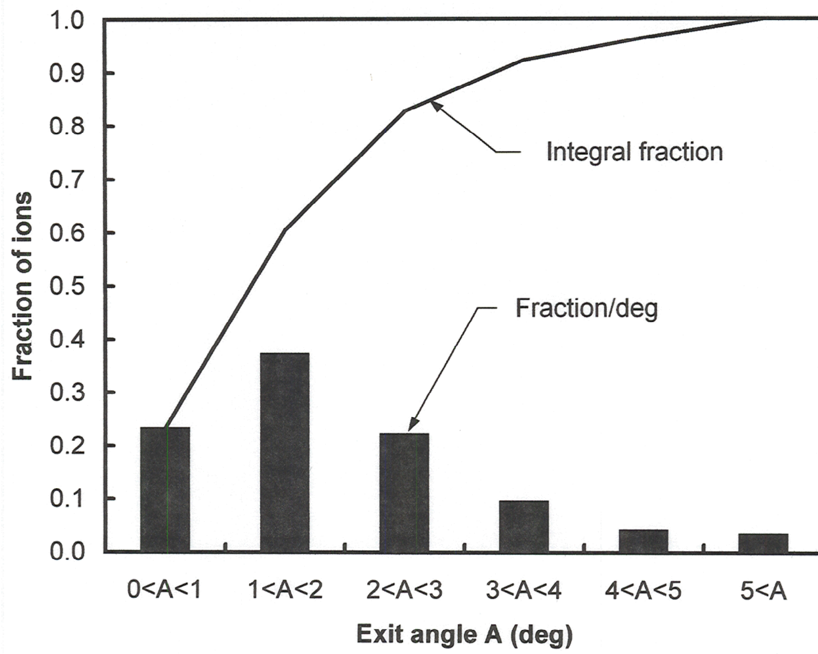

Figure 7(a): Exit angles calculated for 13.6 MeV Xe incident along the surface normal of a 1-μm thick polycarbonate foil.

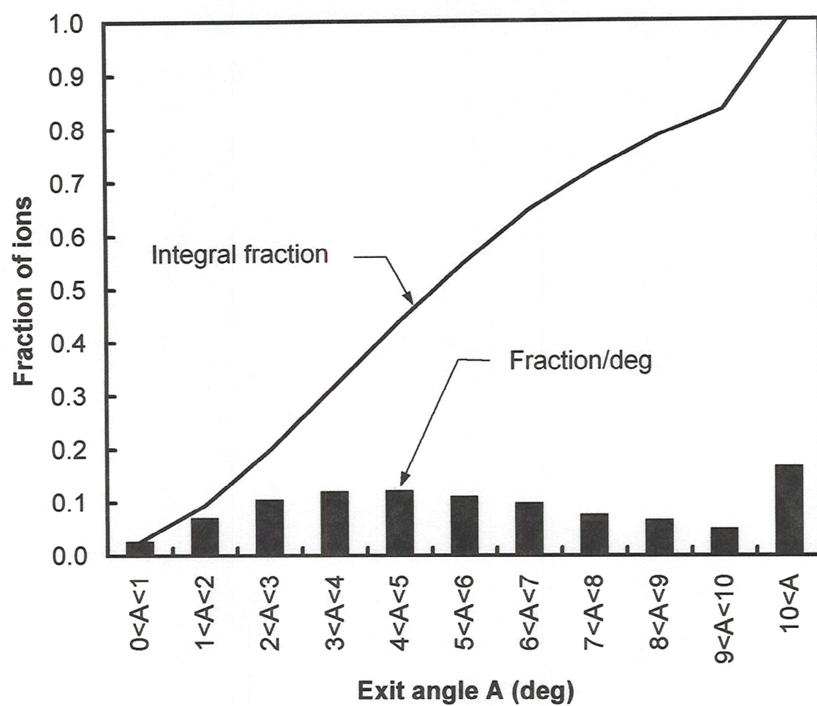

Figure 7(b): Exit angles calculated for 2 MeV Ar incident along the surface normal of a 1-μm thick polycarbonate foil.

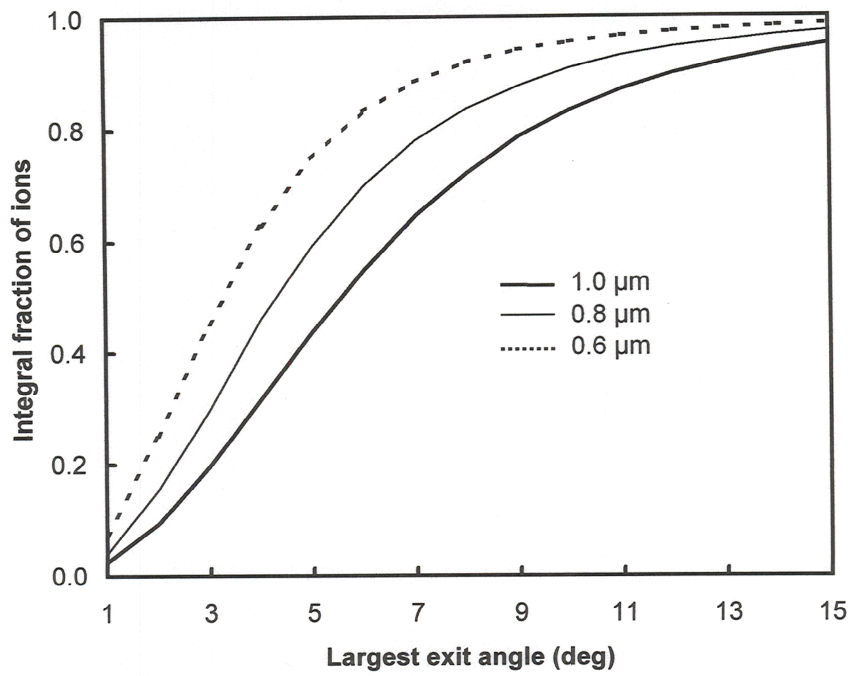

Figure 8: Exit angles calculated for 2 MeV Ar incident along the surface normal of polycarbonate foils with various thicknesses..

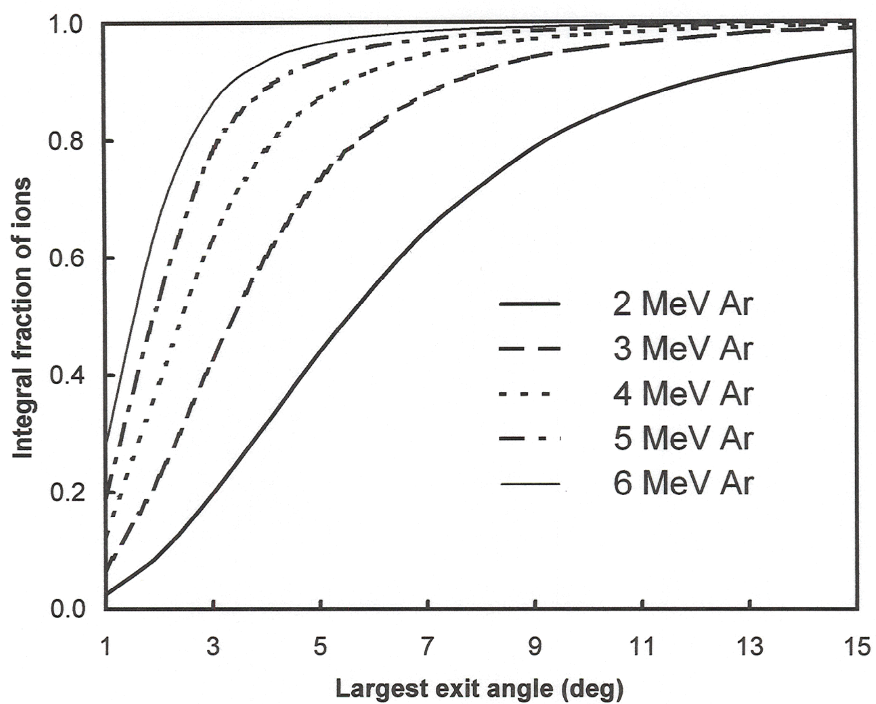

Figure 9: Exit angles calculated for various energies of Ar incident along the surface normal of a 1-μm thick polycarbonate foil.